Hair-Cell Mechanotransduction Persists in TRP Channel Knockout Mice

Xudong Wu[1☯], Artur A. Indzhykulian[1☯], Paul D. Niksch[1], Roxanna M. Webber[1], Miguel Garcia-Gonzalez[2], Terry Watnick[2], Jing Zhou[3], Melissa A. Vollrath[1,4], David P. Corey[1]*

1 Department of Neurobiology, Harvard Medical School and Howard Hughes Medical Institute, Boston, Massachusetts, United States of America, 2 Department of Medicine, Division of Nephrology, University of Maryland, Baltimore, Maryland, United States of America, 3 Renal Division, Department of Medicine, Brigham and Women's Hospital and Harvard Medical School, Boston, Massachusetts, United States of America, 4 Department of Physiology, McGill University Montréal, Québec, Canada

☯ These authors contributed equally to this work.
* dcorey@hms.harvard.edu

Abstract

Members of the TRP superfamily of ion channels mediate mechanosensation in some organisms, and have been suggested as candidates for the mechanotransduction channel in vertebrate hair cells. Some TRP channels can be ruled out based on lack of an inner ear phenotype in knockout animals or pore properties not similar to the hair-cell channel. Such studies have excluded Trpv4, Trpa1, Trpml3, Trpm1, Trpm3, Trpc1, Trpc3, Trpc5, and Trpc6. However, others remain reasonable candidates. We used data from an RNA-seq analysis of gene expression in hair cells as well as data on TRP channel conductance to narrow the candidate group. We then characterized mice lacking functional Trpm2, Pkd2, Pkd2l1, Pkd2l2 and Pkd1l3, using scanning electron microscopy, auditory brainstem response, permeant dye accumulation, and single-cell electrophysiology. In all of these TRP-deficient mice, and in double and triple knockouts, mechanotransduction persisted. Together with published studies, these results argue against the participation of any of the 33 mouse TRP channels in hair cell transduction.

Introduction

Sound conducted to the cochlea causes the movement of stereocilia on hair cells, the receptor cells of the inner ear. Sub-micron deflection of the bundle of stereocilia on a hair cell opens ion channels in microseconds, allowing influx of cations and the generation of a receptor potential [1,2]. Although a great deal is known about the ultrastructure and molecular mechanics of the mechanotransdution apparatus, the molecular identity of the transduction channel has been uncertain.

The physiological properties of this elusive channel provide a fingerprint for screening candidates. The transduction channel is a nonselective cation channel with high permeability to Ca^{2+} (P_{Ca}/P_{Na} = 5–20) [3,4,5]. Although many divalent cations are permeant, they are also channel blockers: the channel can be blocked by Ca^{2+} (IC50 = 1 mM), Mg^{2+}, La^{3+} (4 μm), and

Gd^{3+} (3 µm) [6,7,8]. The single channel conductance varies considerably, ranging from about 80 to 150 pS in 2–3 mM extracellular Ca^{2+}, and is roughly twice that in low Ca^{2+} [6,9,10,11,12]. Some organic cations are also permeant blockers, such as amiloride (IC50 = 50 µm [13]), the fluorescent dye FM1-43 (2 µm [14]) and the antibiotic dihydrostreptomycin (10-70 µM [4,15,16]). The block is voltage dependent indicating that these cations block within the pore, part way along the transmembrane electric field [14,17]. Finally, transduction channels are partially permeable to large organic cations, such as choline and TEA, up to about 12 Å diameter [8]. The current view of the transduction channel shows a funnel-shaped channel with an outer vestibule and 12 Å selectivity filter [8,16,18,19]. These properties suggested that members of the transient receptor potential (TRP) family of ion channels, especially the PKD2 group, would be good candidates for the transduction channel [20,21].

The timing of gene expression provides additional clues. In mice, vestibular hair cells become mechanosensitive beginning on embryonic day 17 (E17) Cochlear hair cells show mechanosensitivity beginning between postnatal day 0 (P0) and P2, in the base and apex respectively [22,23]. We expect mRNA for the transduction channel gene to appear at or slightly before these times. Cuajungco et al. [20] analyzed expression of all 33 TRP channels in a mammalian organ of Corti library, and found 19 TRPs expressed at a single age. Asai et al. [24] went on to analyze expression of mRNAs for all TRP channels in cochlea using RT–PCR from whole inner ear tissue, at E17, E18, P0, P2, P4, P6 and P8 [24]. However, they were unable to distinguish expression in hair cells from that in supporting cells and other surrounding cells, somewhat limiting the usefulness of the analysis.

Here, we explore TRP channels as candidates for the hair cell transduction channel. We take advantage of new data on specific gene expression in hair cells at different developmental time points to narrow the candidates, and further narrow candidates by single-channel conductance and phenotypes in published TRP knockouts. With scanning electron microscopy, FM1-43 loading and single cell physiology, we investigate transduction in mouse knockouts of *Trpm2*, *Pkd2*, *Pkd2l1*, *Pkd2l2* and *Pkd1l3*, and in double and triple knockouts of these genes. We find no substantial deficit in mechanotransduction, ruling out these TRPs. Although many TRPS are expressed in hair cells and surely have important functions, we argue that none of the TRP channels are likely candidates for the transduction channel itself.

Results

To understand specific expression of TRP channels in hair cells, we queried an extensive database of gene expression in hair cells during development [25]. In that study, hair cell- and surrounding cell-specific RNA-seq libraries were prepared from FACS-sorted cochlear and vestibular tissues at E16, P0, P4 and P7. The expression of the TRP channel family for different cell types and ages is shown in Fig 1. The single-channel conductance, drawn from the literature [26,27,28,29,30,31,32,33,34,35,36,37,38,39,40,41,42,43,44,45,46,47,48,49,50,51,52,53,54, 55,56,57,58,59,60,61,62,63,64,65,66,67,68] is also indicated. For reference, S1 Fig shows the TRP family in mouse arranged phylogenetically.

In narrowing candidates, we felt that an attractive transduction channel candidate should show at least two-fold enrichment in hair cells compared to surrounding cells, and it should be expressed in hair cells by the time of transduction onset. It should preferably have a large single channel conductance (>80 pS) although it is possible that a heteromeric TRP channel might have higher conductance than either subunit expressed alone. It would be more attractive if expressed in both auditory and vestibular hair cells [25] and in both inner and outer hair cells in the cochlea [69]. Knockout mice have been generated for a number of TRP channels, and we excluded all TRPs that have been reported to have normal hair cell transduction or showed no phenotype that
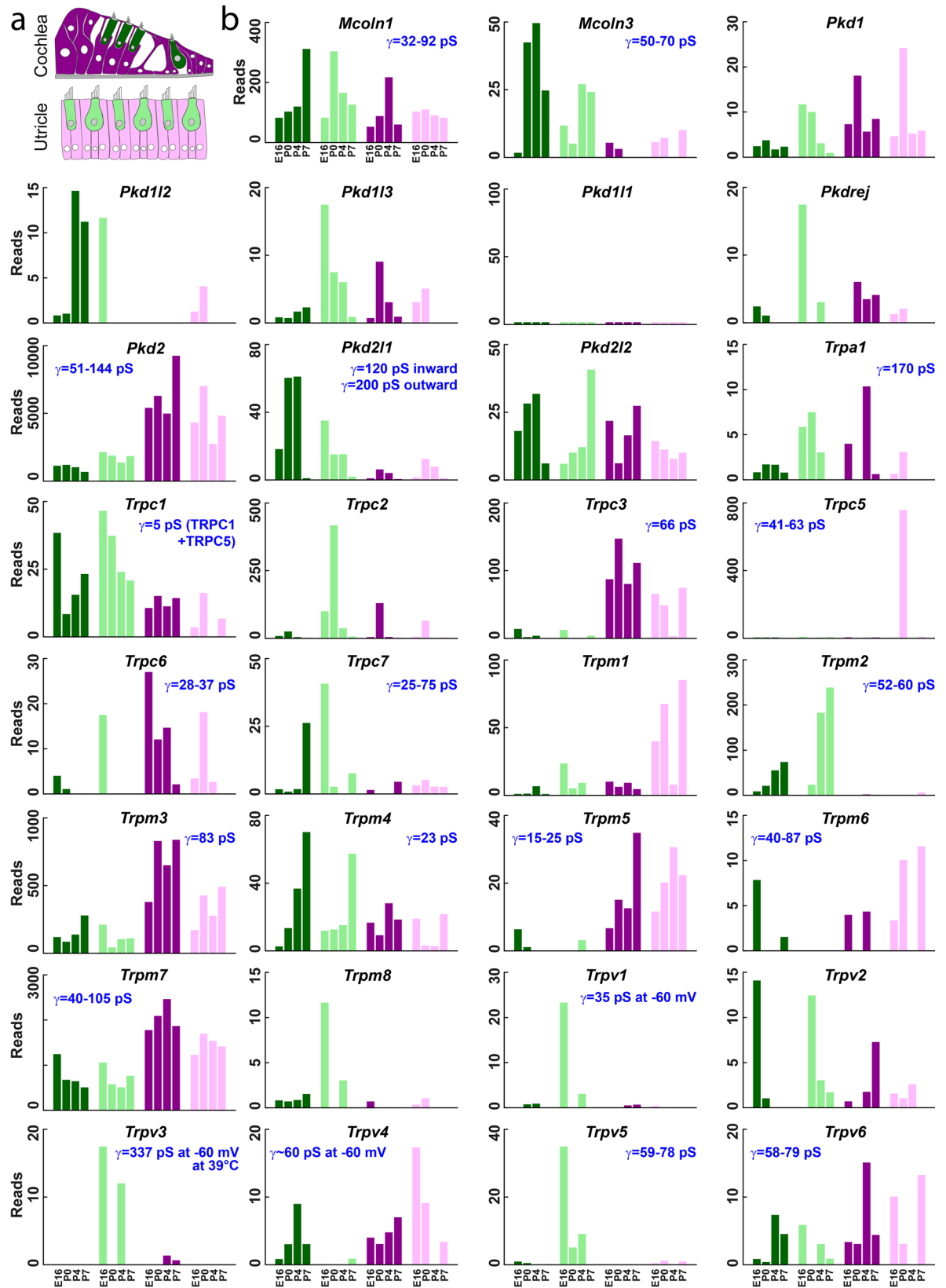
Fig 1. TRP channel expression in cochlear and vestibular hair cells. (a) Schematic of the sorted cells, redrawn from Scheffer et al., 2015 [25]. Hair cells (green) and surrounding cells (purple) were collected from the cochlea (dark colors) and utricle (light colors) at ages E16, P0, P4, and P7. **(b)** Normalized RNA-seq read counts in hair cells and surrounding cells (colors

as in **a**). Data are shown for 31 of the 33 members of the TRP channel family in mouse. *Mcoln2* and *Trpc4* showed negligible counts in all samples. Data from www.shield.hms.harvard.edu [25].

might be expected from auditory or vestibular deficits. In mice, loss of vestibular function often leads to circling, spinning or head-bobbing behavior. Such behavior is often the first indication of an inner-ear phenotype in random or targeted mutagenesis and is usually noted in phenotypic descriptions. Auditory function is usually tested only if there is a reason to suspect dysfunction, for instance if vestibular problems are noted. Trpa1, Trpc1, Trpc3, Trpc5, Trpc6, Trpv4, Trpml3 and Trpm1 can be excluded on this basis [70,71,72,73,74]. Similarly, channels with a reported conductance <80 pS were excluded unless other strong indications were present.

Trpm2 is not required for hair cell transduction

Based on these criteria, we first focused on *Trpm2*. Its mRNA shows 90-fold enrichment in hair cells compared to surrounding cells, and it is first expressed at E17 in vestibular system and P0 in cochlea, matching the onset of mechanosensitivity. Expression further increases during development in both tissues. Although the published conductance of 50–60 pS is somewhat below our criterion, the expression pattern warranted further investigation.

We therefore generated a conditional *Trpm2* knock-out mouse in which exon 21—encoding the fifth transmembrane and pore domains of Trpm2—is flanked by LoxP sites (*Trpm2*fl/fl; see Methods and S2 Fig). *Trpm2*fl/fl mice were viable and could be bred as homozygotes. For hair-cell-specific Cre-mediated recombination, we crossed *Trpm2*fl/fl mice with mice expressing Cre-recombinase under control of the *Gfi1* promoter [75]. PCR from genomic DNA purified from inner ears of *Trpm2*fl/fl:*Gfi1*-Cre+/- mice confirmed the deletion.

*Trpm2*fl/fl:*Gfi1*-Cre+ homozygous knockout mice looked similar to their *Trpm2*fl/+: *Gfi1*-Cre+/- heterozygous control littermates, suggesting no gross developmental defects. *Gfi1* is expressed in vestibular hair cells, so Cre recombination should delete *Trpm2* in these cells, however *Trpm2*-deficient mice showed no obvious vestibular deficit.

To test mechanotransduction in *Trpm2*-deficient cochlear hair cells, we applied FM1-43 dye [76] to cultured organ of Corti explants. Both control and *Trpm2*-deleted hair cells accumulated FM1-43, showing similar levels of fluorescence intensity, suggesting that mechanotransduction persisted in the absence of *Trpm2* (Fig 2A). To further test transduction, we recorded hair cell transduction currents in response to a family of bundle deflections. Both wild-type and *Trpm2*fl/fl:*Gfi1*-Cre+ outer hair cells showed high amplitude, rapidly adapting transduction currents (Fig 2B), with peak currents in response to the largest deflections that were not significantly different (Fig 2C).

The auditory brainstem response (ABR), a sound-evoked voltage change measured near the brainstem, tests both transduction and synaptic function of the peripheral auditory system. ABR responses to pure tone stimuli were largely normal in *Trpm2*-deleted animals (Fig 2D). There was a slight elevation of hearing threshold at high frequencies in *Trpm2*-deficient mice, but overall auditory function was preserved. Based on these results we conclude that Trpm2 is not required for hair cell transduction.

Pkd2, *Pkd2l1*, *Pkd2l2*, and *Pkd1l3* are not individually required for hair cell transduction

Pkd2l1 also showed an intriguing expression pattern (Fig 1), with 6.3-fold enrichment in hair cells compared to surrounding cells in both cochlea and utricle. The reported conductance of Pkd2l1 channels, 120–200 pS [28,67], matched that expected for the transduction channel.
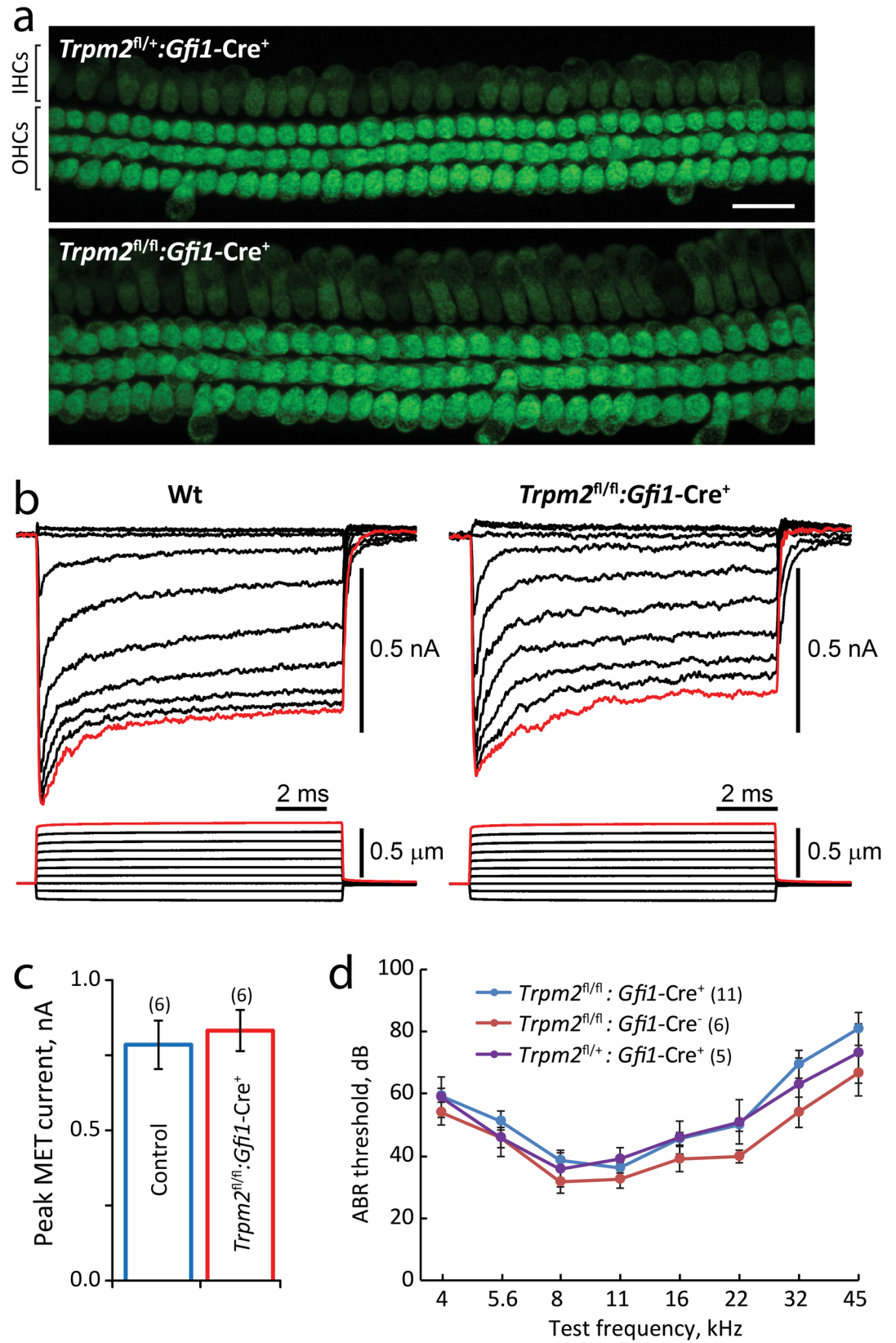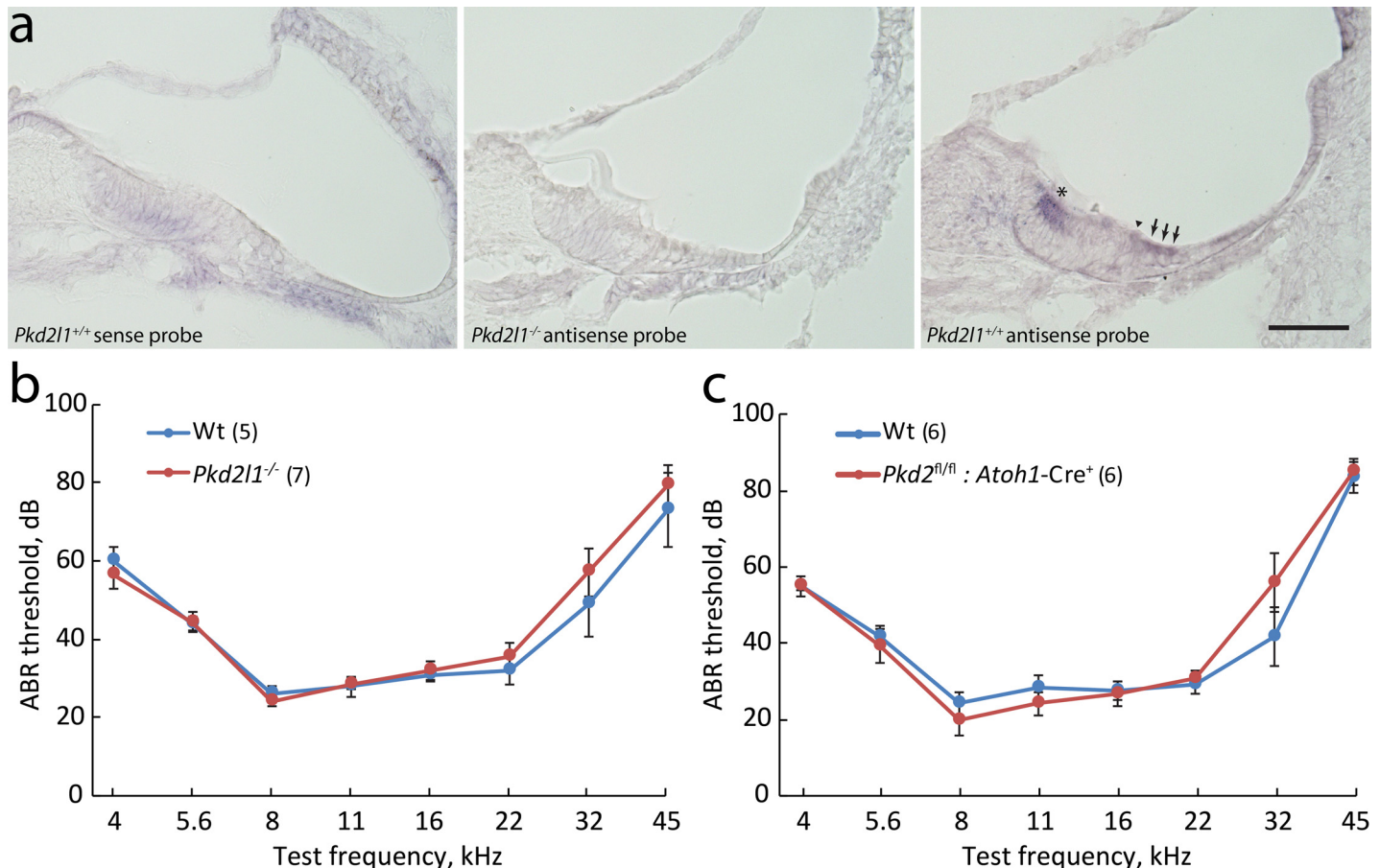
Fig 2. Trpm2 is not required for hair cell mechanotransduction. (a) FM1-43 accumulation by IHCs and OHCs from control *Trpm2*fll+:*Gfi1*-Cre+ mice *(top)* and deleted *Trpm2*fl/fl:*Gfi1*-Cre+ mice *(bottom)*. FM1-43 accumulation by hair cells was similar in control and *Trpm2*-deleted hair cells. Age: P5+2div. Scale bar = 20 μm. **(b)** A family of OHC transduction current recordings *(top traces)* in response to stereocilia bundle deflections *(bottom traces)* in WT *(left)* and *Trpm2*fl/fl:*Gfi1*-Cre+ *(right)* mice. **(c)** Average peak transduction current (red traces in **b**) for control mice (WT and *Trpm2*fl/+:*Gfi1*-Cre+) and *Trpm2*fl/fl:*Gfi1*-Cre+ mice. **d,** ABR thresholds in response to pure tone stimuli. *Trpm2*fl/fl: *Gfi1*-Cre+ mice show normal hearing. Data are mean ± sem; n as indicated.

Indeed, the PKD2 group of TRP channels has previously been suggested to include attractive candidates for the transduction channel [21].

We obtained a *Pkd2l1* knockout mouse lacking exons 3 and 4, which produced a premature stop in exon 5 [77]. Using *in situ* hybridization in cochlear sections, an antisense probe showed label in the hair-cell region (Fig 3A). No expression of *Pkd2l1* mRNA was detected in *Pkd2l1*−/− mice, confirming the knockout, or with sense probe, confirming the probe specificity. However ABR measurements in *Pkd2l1*−/− mice showed normal hearing thresholds (Fig 3C), indicating that mechanotransduction persists in the absence of Pkd2l1. In scanning electron microscopy (SEM) images of *Pkd2l1*−/− mice at age P35, hair bundles appeared normal compared to wild-type controls (Fig 4A, 4C, 4E and 4G).

Fig 3. Neither *Pkd2* nor *Pkd2l1* is required for hair cell mechanotransduction. (a) *In situ* hybridization in cochlear sections. *(Left)* no label is evident with a control sense probe. *(Middle)* no specific label is evident in the *Pkd2l1* knockout. *(Right)* *In situ* hybridization with an antisense probe shows label of inner hair cells (arrowhead), outer hair cells (arrows) and inner sulcus cells (asterisks) in the organ of Corti. Scale bar = 50 μm; age P2. **(b)** ABR thresholds in response to pure tone stimuli. *Pkd2l1*−/− mice show normal hearing at age P31-P37. **(c)** *Pkd2*−/−:*Atoh1*-Cre+/−mice show normal hearing at age 4~6 weeks. Data are mean ± sem; n as indicated.

The PKD2 group of TRP channels is not very divergent ([S1 Fig](#)), and PKD2 channels interact with each other forming heteromultimeric channels, further indicating their similarity [78,79,80,81]. These both raise the possibility that expression of *Pkd2* or *Pkd2l2* might compensate for the loss of *Pkd2l1*.

We therefore generated a conditional *Pkd2* knock-out mouse line, by flanking exon 9 (aa630-671, comprising the pore and most of the sixth transmembrane domain) with loxP sites *Pkd2*$^{fl/fl}$; see [Methods](#) and [S3 Fig](#)). Hair-cell-specific Cre recombination was achieved by crossing *Pkd2*$^{fl/fl}$ mice with a mouse line expressing Cre recombinase under control of the *Atoh1* enhancer, restricting the Cre expression to hair cells [82]. Hair cell-specific absence of *Pkd2* expression in *Atoh1*-Cre mice was confirmed using inner ear genomic PCR ([S3 Fig](#)).

We first assessed the consequence of *Pkd2* deletion alone. *Pkd2*$^{fl/fl}$:*Atoh1*-Cre$^+$ knockout mice looked similar to their heterozygous control *Pkd2*$^{fl/+}$:*Atoh1*-Cre$^+$ littermates, suggesting no gross developmental defects. Hair bundles in *Pkd2* knockouts also appeared normal ([Fig 4B–4F](#)). ABR measurements showed normal hearing thresholds ([Fig 3D](#)), indicating that hair-cell mechanotransduction does not require *Pkd2*.

As an independent confirmation, we used a second *Pkd2*$^{fl/fl}$ mouse line [83] missing exons 11–13, and deleted *Pkd2* in hair cells by crossing to *Atoh1*-Cre$^+$. In heterozygous controls, an antibody to Pkd2 labeled the kinocilia of hair cells and the primary cilia of adjacent supporting cells ([S4 Fig](#)). In homozygous knockouts, antibody label was missing from kinocilia but not adjacent primary cilia, confirming both the antibody specificity and the cell-specific deletion. These *Pkd2* knockouts have normal hearing as well ([S4 Fig](#)).

We then obtained *Pkd2l2* knockout mice in which exons 3 and 4 were replaced with a LacZ +Neo cassette, terminated by a stop (Jackson Laboratory B6.129P2- *Pkd2l2*tm1Dgen/J, Stock #: 005829). Because Pkd2l1 was thought to function together with Pkd1l3 in acid taste transduction [84,85,86], we also obtained a *Pkd1l3* knockout line in which deletion of exons 17 through 21 produces a frame shift [87].

In double knockouts, we assessed stereocilia bundle morphology with SEM, and hearing sensitivity with ABR. Double knockout mice with hair cells missing both *Pkd2* and *Pkd2l1* showed normal bundles ([Fig 4D–4J](#)) and had normal hearing thresholds ([Fig 4M](#)). Similarly, single *Pkd1l3* knockouts and double knockouts missing both *Pkd2l1* and *Pkd1l3* showed normal bundles ([Fig 4H and 4I](#)) and normal hearing thresholds ([Fig 4N](#)). Single *Pkd2l2* knockouts are also normal ([Fig 4K–4O](#)).

Triple *Pkd2*, *Pkd2l1* and *Pkd2l2* knockout mice show normal transduction

Pkd2$^{fl/fl}$:*Atoh1*-Cre$^+$, *Pkd2l1*$^{-/-}$ and *Pkd2l2*$^{-/-}$ mouse lines were then crossed to each other to generate triple knockout mice. Triple knockouts were viable and could be bred as homozygotes. SEM imaging of stereocilia bundles revealed normal bundle morphology in adult mice ([Fig 4L](#)). To test transduction in cochlear hair cells missing *Pkd2*, *Pkd2l1* and *Pkd2l2*, we first used the FM1-43 dye accumulation assay in acutely dissected P6 organ of Corti epithelia. Triple knockout mice showed similar levels of fluorescence dye intensity accumulation in hair cells as compared to double knockout control mice, suggesting preserved transduction ([Fig 5A](#)). To further test transduction, we recorded transduction currents in response to a family of bundle deflections in triple knockout organ of Corti explants and in age-matched control wild-type mice of the same background. Both wild-type and *Pkd2*$^{fl/fl}$:*Atoh1*-Cre$^+$:*Pkd2l1*$^{-/-}$:*Pkd2l2*$^{-/-}$ OHCs showed high amplitude, rapidly adapting transduction currents ([Fig 5B](#)). The peak transduction current in response to the largest deflection was similar between the tested groups ([Fig 5C](#)). Vestibular hair cells of *Pkd2*$^{fl/fl}$:*Atoh1*-Cre$^+$:*Pkd2l1*$^{-/-}$:*Pkd2l2*$^{-/-}$ triple knockouts also
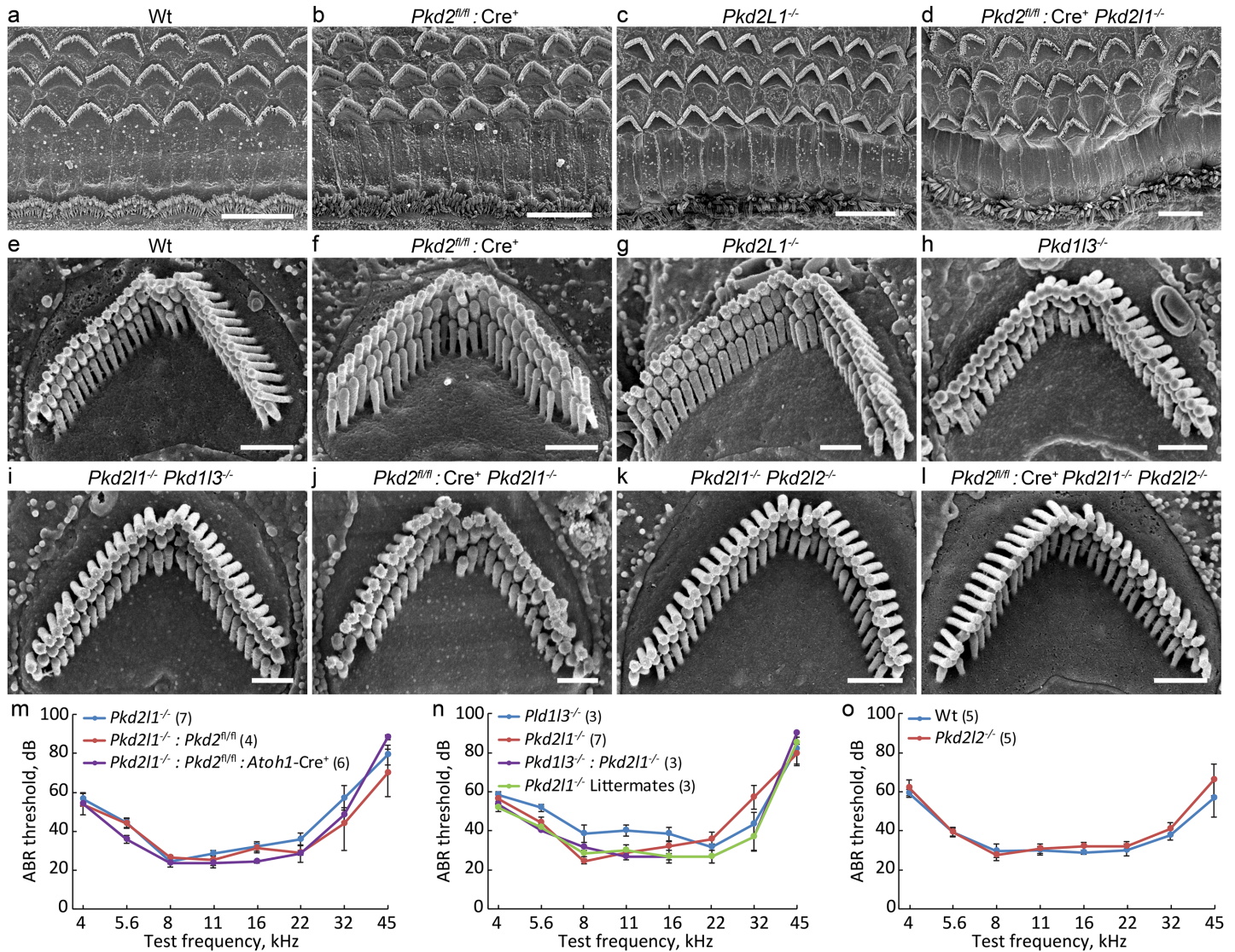
Fig 4. Mice lacking single or multiple PKD genes show normal stereocilia bundle morphology and hearing function. (a-d) SEM images of postnatal 4~6 weeks organ of Corti hair cells at low magnification in WT and PKD-deficient mice. Scale bar = 10 μm. **(e-l)** OHC bundles at high magnification. Scale bar = 1 μm. **(m)** ABR thresholds in response to pure tone stimuli in *Pkd2* and *Pkd2l1* single and double knockouts. **(n)** *Pkd2l1* and *Pkd1l3* single and double knockouts. **(o)** *Pkd2l2* knockouts. No functional deficit was observed in any combination tested. Data shown as mean ± sem.

doi:10.1371/journal.pone.0155577.g004

showed transduction currents (data not shown). ABR responses to pure tone stimuli showed similar threshold levels in $Pkd2^{fl/fl}$:$Atoh1$-Cre$^+$:$Pkd2l1^{-/-}$:$Pkd2l2^{-/-}$ triple knockouts, as compared to their double knockout littermates with either $Pkd2$ or $Pkd2l2$ present (Fig 5D). Based on these results we conclude that the PKD2 subfamily of channels is not required for hair cell transduction.

Discussion

The TRP channel family is broadly expressed in a different cell types and activated by a variety of stimuli, being especially prominent in reception of sensory stimuli. Like the hair-cell transduction channel, they are generally nonselective cation channels of high conductance. Some TRPs are thought to sense mechanical stimuli [88,89], although activation may be indirect
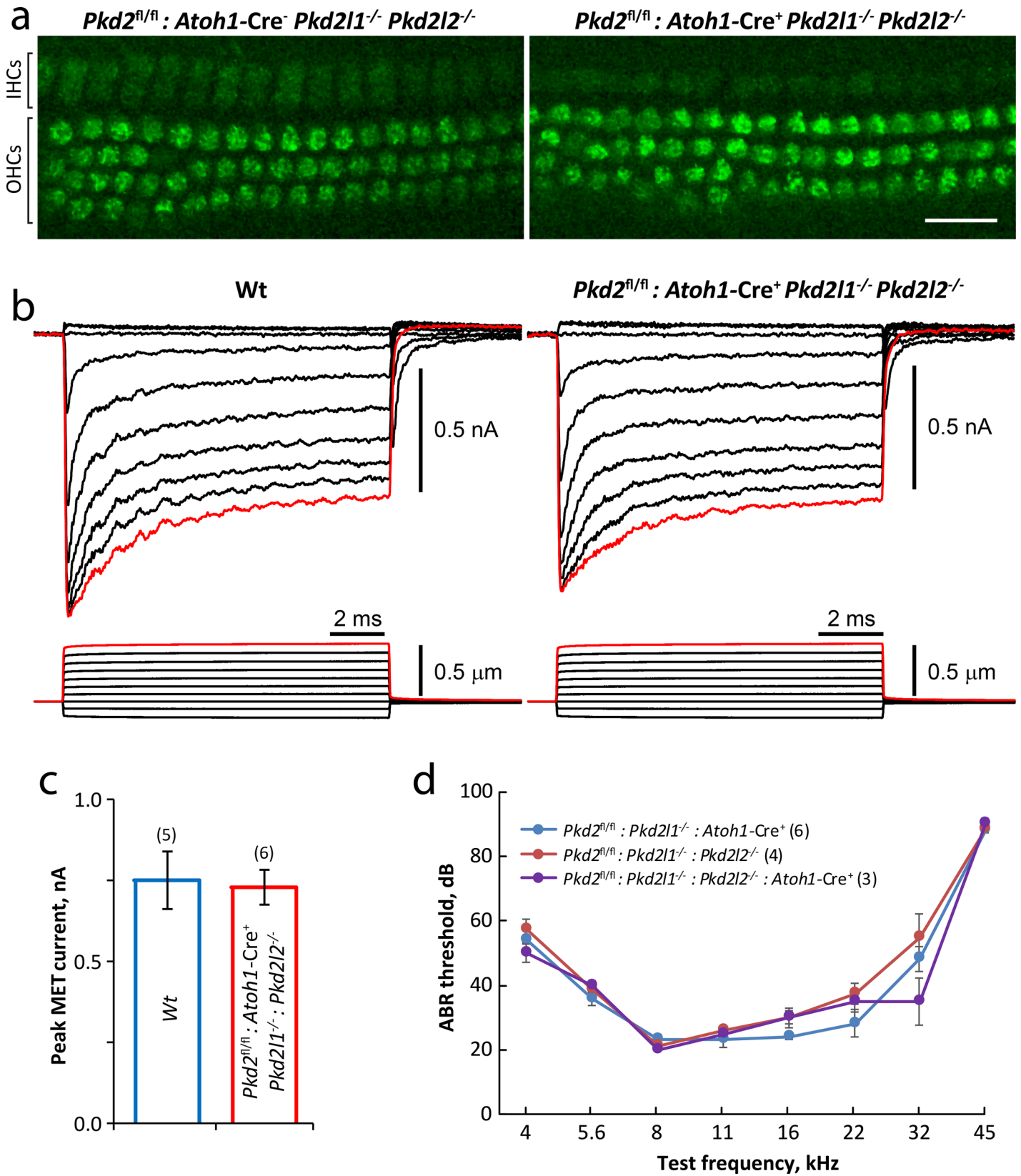
Fig 5. Triple PKD knockout (*Pkd2*^{fl/fl}:*Atoh1*-Cre⁺:*Pkd2l1*^{-/-}:*Pkd2l2*^{-/-}) mice show normal mechanotransduction and normal hearing in ABR measurements. (a) FM1-43 accumulation is similar in IHCs and OHCs from P6 *Pkd2*^{fl/fl}:*Atoh1*-Cre⁻:*Pkd2l1*^{-/-}:*Pkd2l2*^{-/-} controls lacking Cre *(left)* and *Pkd2*^{fl/fl}:*Atoh1*-Cre⁺:*Pkd2l1*^{-/-}:*Pkd2l2*^{-/-} knockout mice *(right)*, suggesting normal transduction. Scale bar = 20 μm. **(b)** A family of OHC transduction currents *(top traces)* in response to stereocilia bundle deflections *(bottom traces)* in WT *(left)* and *Pkd2*^{fl/fl}:*Atoh1*-Cre⁺:*Pkd2l1*^{-/-}:*Pkd2l2*^{-/-} knockout *(right)* mice. **(c)** Average peak transduction currents (red traces in **b**) for WT mice (blue; n = 5) and triple knockout (red bar, n = 6). **(d)** ABR threshold measurements in response to pure tone stimuli in *Pkd2*^{fl/fl}:*Atoh1*-Cre⁺:*Pkd2l1*^{-/-}:*Pkd2l2*^{-/-} knockout mice indicate normal hearing. Data are mean ± sem.

[90]. This has led to the consideration of various TRPs as components of the hair cell mechanotransduction channel. Here we evaluate each of the six branches of the TRP family in mice.

TRPMLs

The varitint-waddler mutant (Va(J)) of *Trpml3* (mucolipin 3; *Mcoln3*) has profound hearing loss [91] and impaired transduction in hair cells [64,92]. However, it was found that the Va(J) mutation leads to constitutive activation of the channel, causing a continuous inward current and consequent cell death. Hearing loss is explained by the loss of hair cells [20,61,63,64,92]. Hearing is normal in a null mutant of *Trpml3* [93].

The TRPML branch is not very divergent (S1 Fig) so there is the possibility of compensation for loss of *Trpml3* by a related gene. *Trpml2* has negligible expression in the inner ear, but *Trpml1* is expressed in both hair cells and surrounding cells (Fig 1). However the channel conductance for this branch is not consistent with the transduction channel conductance, and Trpml1 protein is mainly located in late endosomes and lysosomes [94].

PKDs

An analysis of candidates for the hair cell transduction channel pointed out that some members of the PKD (TRPP) branch of the TRP family have properties similar to those of the transduction channel [21]. PKD2 channels are highly permeable to calcium: Pkd2 has a P_{Ca}/P_{Na} of 5 whereas Pkd2l1 has a P_{Ca}/P_{Na} of ~4 [95]. The portfolio of blocking ions is similar to that of hair cells: Pkd2 is blocked by Ca^{2+}, La^{3+} and Gd^{3+}, and Pkd2l1 is blocked by Ca^{2+}, Mg^{2+}, La^{3+} and Gd^{3+}. Both Pkd2 and Pkd2l1 are blocked by amiloride (IC50 = 40–130 μm). The conductance of Pkd2 is 40–170 pS [40,48], and Pkd2l1 conductance is ~120 pS for inward current [67,96]. *Pkd2*, *Pkd2l1* and *Pkd2l2* are all expressed in hair cells, with the *Pkd2l1* profile being especially appropriate [25]. Moreover, some studies have suggested that the Pkd2 channel is mechanosensitive—specifically that it is located in primary cilia, where it is activated by cilia bending from environmental fluid flow [97,98,99].

Because constitutive deletion of the *Pkd2* gene is embryonic lethal, we used an *Atoh1*-Cre line to delete *Pkd2* conditionally in hair cells. Using a pure-tone ABR test, we found that hearing is normal in *Pkd2* conditional knockout mice (Fig 3D). SEM imaging showed a normal hair bundle in the cochlea. Testing a second, independent *Pkd2* conditional knockout line which truncates the C-terminal of Pkd2 channels, we found similarly normal function. Furthermore, antibody labeling showed that in hair cells Pkd2 is located in the kinocilia but not stereocilia. Finally, we recently re-analyzed mechanosensitivity in primary cilia in a variety of cell types and found that none shows rapid influx of Ca^{2+} upon cilium bending, casting doubt on the idea that Pkd2 is a mechanically gated channel [67,96,100].

We also investigated if Pkd2l1 is involved in hair cell transduction, using a *Pkd2l1* knockout mouse that we recently described [77]. RT-PCR from whole mouse cochlea showed that expression of *Pkd2l1* is correlated with the acquisition of mechanotransduction [24], and RNA-seq showed it is specifically expressed in hair cells at the start of mechanosensitivity (Fig 1). A sensitive mass spectroscopy study found that Pkd2l1 protein is enriched in hair bundles

of the chicken auditory epithelium [101]. In situ hybridization in mouse showed that *Pkd2l1* is highly expressed in hair cells and also some inner sulcus cells (Fig 3A). However the *Pkd2l1* knockout mouse did not show abnormalities in hearing, using the ABR test (Fig 3C), or abnormal hair bundle morphology (Fig 4).

Pkd1l3 had been thought to form a heteromeric complex with Pkd2l1 for sour taste sensation [85,102,103], suggesting that it might share function with Pkd2l1 in hair cells. *Pkd1l3* was also found to be expressed in the auditory system [24], although expression in hair cells is limited (Fig 1). However we found that a single knockout of *Pkd1l3* and a double knockout with *Pkd2l1* showed no abnormalities in the ABR or hair bundle morphology (Fig 4).

Pkd2l2 is also expressed in hair cells, although not preferentially (Fig 1). We found that a single *Pkd2l2* knockout has a normal hearing sensitivity and hair bundle morphology. Because of the possibility of compensation among this closely-related group, we created double and triple knockouts of *Pkd2*, *Pkd2l1* and *Pdk2l2*. Even triple knockouts showed no deficit in hearing sensitivity, bundle morphology, or mechanotransduction assessed with FM1-43 accumulation and single-cell recording. We can thus rule out the PKD2 branch of the TRP family.

In addition to *Pkd1l3*, some of the *Pkd1* group of TRPs are sparsely expressed in hair cells. However none of the *Pkd1* group have robust and hair-cell-specific expression profiles (Fig 1). *Pkd1* mutants have normal transduction current and only moderate loss of hearing sensitivity [104]. Moreover, PKD1s are thought to form ion channels as heteromultimers with PKD2 channels [105], and the PKD2s have been ruled out.

The entire PKD group of TRP channels is thus unlikely to participate in hair-cell transduction.

TRPA

Trpa1 was also considered as a strong transduction channel candidate because knockdown of expression in both mice (with virally delivered siRNA) and zebrafish (morpholino injection) reduced the transduction current, and because it has a large single-channel conductance of 250 pS in low Ca^{2+} [106], (data not shown). However, mice lacking *Trpa1* have normal transduction current and hearing [70]. *Trpa1* is the only member of the *Trpa* branch in mice, so compensation by a related gene is unlikely.

TRPCs

Although *Trpc1* is expressed in mouse hair cells (Fig 1), the other members of this branch do not have an appropriate expression pattern and *Trpc4* is not expressed at all. In addition, a quadruple knockout of *Trpc1*, *Trpc3*, *Trpc5* and *Trpc6* shows normal hearing sensitivity and hair cell morphology [71,72]. We previously showed that the remaining TRPC gene, *Trpc2*, is highly expressed in mouse vomeronasal neurons and the protein is located in the sensory cilia where it is thought to participate in pheromone transduction [107]. *Trpc2* knockout mice do lack pheromone sensitivity but have no vestibular deficit [108]. Also, *TRPC2* is a nonfunctional pseudogene in a species (human) that has normal hearing [109]. Finally, the single channel conductance of the TRPC channels is lower than that of the hair cell transduction channel.

TRPMs

In situ hybridization and RNA-seq showed *Trpm2* to be selectively expressed by inner ear hair cells, suggesting that it plays an important role in these cells [25]. We found, however, that *Trpm2* knockout mice exhibited normal transduction current and FM-143 accumulation. *Trpm1* knockouts also have normal hearing [73]. It might be that other TRPMs compensate in these knockouts, but—with the exception of *Trpm7*—none of the others has an appropriate

expression pattern or single-channel conductance. *Trpm*7 is expressed but not enriched in hair cells, its single channel conductance is high but not as high as the transduction channel, and zebrafish studies suggest it is not required for hair cell transduction in zebrafish [110]. Thus none of the TRPMs seems likely to be a transduction channel.

TRPVs

Trpv4 was first suggested as a possible component of a heteromeric transduction channel because it was mechanosensitive—responding to changes in osmolarity—and was expressed in auditory hair cells [111]. Newer methods have shown the *Trpv4* gene to be expressed only at very low levels in cochlear hair cells and not at all in utricular hair cells [25]. Although *Trpv4* knockout mice show mild, late onset hearing loss, there is no deficit in hearing at earlier ages, excluding it as a transduction channel candidate [72].

Of other TRPVs, only Trpv3 has a large conductance; however its expression pattern is not consistent with the hair cell transduction channel (Fig 1). None of the other TRPV channels shows an appropriate expression pattern in hair cells.

Conclusion

Although the TRP family of ion channels initially seemed like a rich source of candidates for the hair-cell transduction channel, most of them can be ruled out by inappropriate expression pattern, inappropriate conductance, or lack of an auditory or vestibular phenotype in knockout mice. Here, we have tested the remaining reasonable candidates—including some that were quite attractive based on expression and conductance—but found no deficit in transduction in hair cells of these animals. Although many TRPs are expressed in hair cells and many are sure to carry out important functions in these cells, it now seems safe to exclude the entire TRP family in the search for a transduction channel.

Materials and Methods

TRP channel expression data

Expression data for all 33 mouse TRP channels were drawn from Scheffer et al., 2015, as posted on the SHIELD database (shield.hms.harvard.edu). Read counts were analyzed based on the 20207 RefSeq genes in the DNAnexus set. Pkd1l1 is not in that set, so reads for Pkd1l1 were identified by specifically querying the raw data set.

Mouse lines

This study was carried out in strict accordance with the recommendations in the Guide for the Care and Use of Laboratory Animals of the National Institutes of Health. The protocol was approved by the Institutional Animal Care and Use Committee at Harvard Medical School (Protocol Number: 03524). ABR measurements were performed under anesthesia (ketamine (100 mg/kg)/xylazine (10 mg/kg) cocktail). Newborn mice (P0-P4) were anesthetized by cooling, then euthanized by decapitation. Adult mice were euthanized by isoflurane overdose, followed by cervical dislocation. All efforts were made to minimize suffering. All primers used in current study are summarized in **Table 1**.

Trpm2 **conditional knockout mouse line.** We worked with Ingenious Targeting Laboratory (Ronkonkoma, New York, USA) to make the *Trpm2* conditional knockout. A 10.2-kb *Trpm2* genomic fragment was subcloned from a C57BL/6 BAC clone to construct the targeting vector using homologous recombination. A FRT-LoxP-Neo-FRT-LoxP cassette was inserted upstream of exon 21 and the third single LoxP site was inserted downstream of exon 21 (S2

Table 1. Primers used for genotyping and validation of gene deletion.

Mouse lines	Primer Name	PCR primer concentration	Sequence	Floxed allele	WT allele	KO allele	Purpose
Trpm2cKO (David Corey)	LOX	1.2 µM	TGAGGCGGAAGGAATTAGCAC	320	259		Genotyping
	SDL	1.2 µM	CCCACCTGACAGTCACAAGTGTG	320	259		Genotyping
	TM2cKO15101f	1.2 µM	GACTTCATCATGTTCTGTCT	4184 (N/A*)	2415 (N/A*)	616	Verification cKO in the inner ear
Pkd2cKO (Jing Zhou)	mPKD2in9F3	0.6 µM	TTGTGCATTTGGTGATGTGTTA	520	468		Genotyping
	mPKD2in9R3	0.6 µM	CCACATTTACATGGCATCTGAG	520	468		Genotyping
	PKD2-5940f1	1.2 µM	AAGCTGTGTTATCATTCTAGAAAGC	>2457	2457	344	Verification cKO in the inner ear
Pkd2cKO (Terry Watnick)	MG/3 flox c-f	1.2 µM	GGGGTTTCCTATGAAGAGTTCCAAG	485	396		Genotyping
	MG/3 flox d-r	1.2 µM	CTGACAGGCACCTACAGAACAGTG	485	396		Genotyping
Pkd2l1	Neo82	0.6 µM	CTGCCTTGGGAAAAGCGCCT		~520	~480	Genotyping
	MPclF904	0.6 µM	AAGATCAGCTCCCCTTTGGACCT		~520	~480	Genotyping
	R520	0.6 µM	TTCCACCCCAGGATTCTCTG		~520	~480	Genotyping
Gfi1-Cre	Gfi-1F	1.2 µM	GGG ATA ACG GAC CAG TTG		609	672	Genotyping
	Gfi1Cre-R	1.2 µM	GCC CAA ATG TTG CTG GAT AGT		609	672	Genotyping
	Gfi-1R	0.6 µM	CCG AGG GGC GTT AGG ATA		609	672	Genotyping
Atoh1-Cre	Atoh1Cre-F	1.2 µM	ATCGGCCTCCTCCTCGTAGACAGC			550	Genotyping
	Atoh1Cre-R	1.2 µM	GGATCCGCCGCATAACCAGTGA			550	Genotyping
Pkd2l2	IMR4245	0.3 µM	CATCATCAGGTAGAGAAGTGTCCAC		~200	~450	Genotyping
	IMR4246	1.2 µM	CGTGCGTGCAAACACCCACACACAG		~200	~450	Genotyping
	IMR5100	1.2 µM	TTCAACAGACCTTGCATTCCTTTGG		~200	~450	Genotyping
Pkd1l3	1111nF-5'	0.3 µM	AGGAGAGGATTGACTTCTATGAG		~250	650	Genotyping
	1112nR-5'	0.3 µM	CAGGAGAGCCTCTGGACTCGTGT		~250	650	Genotyping
	1328F-5'	1.2 µM	GATGGAAGCCGGTCTTGTCGAT		~250	650	Genotyping
	1538R-5'	1.2 µM	TCGAGCCCCAGCTGGTTCTTTCC		~250	650	Genotyping

* Not amplified

Fig). The region flanked by the second and the third LoxP sites is about 2.0 kb. Exon 21 encodes amino acids 929–985 and corresponds to the fifth transmembrane domain and pore of *Trpm2*; its deletion also causes an early stop. A homology short arm extends 1.8 kb to the 3' of the FRT-LoxP-Neo-FRT-LoxP cassette whereas a homology long arm extends 6.4 kb from the 5' side of the third LoxP site. The linearized targeting vector was then electroporated into iTL BA1(C57BL/6X129/SvEv) hybrid embryonic stem cells.

Pkd2l1 constitutive knockout. We have previously described the *Pkd2l1* knockout [77]. It lacks exons 3 and 4, leading to a premature stop codon in exon 5.

Pkd2 conditional knockout. A 7.3kb genomic fragment of the *Pkd2* gene was used to construct the targeting vector. Three LoxP sites were inserted as shown in S3 Fig. The first LoxP site was inserted upstream of exon 9 and a LoxP-Neo-LoxP cassette was inserted downstream of exon 9. The first and second LoxP sites thus flank a 2.2kb genomic region that includes exon 9. Exon 9 encodes amino acids 630–671, comprising the pore and most of the sixth transmembrane domain of Pkd2. The homology short arm extended 0.9 kb to the first loxP site and a homology long arm extended 4.2 kb downstream of the LoxP-Neo-LoxP cassette.

Pkd2l2 constitutive knockout. Mice were obtained from The Jackson Laboratory (B6.129P2-*Pkd2l2*^tm1Dgen/J, #005829). In this mutant mouse line, a lacZ-Neo cassette was

inserted into the *Pkd2l2* gene to replace a 1.8-kb genomic fragment including exons 3 and 4. As a result, the endogenous *Pkd2l2* gene promoter drives expression of the beta-galactosidase gene but not the endogenous *Pkd2l2* gene (S5 Fig).

Pkd1l3 constitutive knockout. Mice were obtained from The Jackson Laboratory (B6;129S4-*Pkd1l3*tm1Sul/J, Stock #: 008419). They lack exons 17 through 21, which encode transmembrane domains 2–5 [87].

Cre lines. The *Gfi1-Cre* mouse line was generously provided by Dr. Lin Gan (University of Rochester)[75]. The *Atoh1-Cre* mouse was obtained from The Jackson Laboratory (B6.Cg-Tg (*Atoh1-cre*)1Bfri/J, #011104) [82].

Immunofluorescence

Mouse cochleas and/or utricles were dissected from P2~P8 mutant mice and their wild-type littermates. Samples were fixed with 4% formaldehyde for 2 hr, rinsed with PBS, incubated in 0.1 M citrate buffer (pH 7.0) at 60°C for 30 min for antigen retrieval. Whole mount samples were permeabilized with 0.5% Triton X-100 for 30 min, and blocked with 10% goat serum supplemented with 0.5% Triton X-100 for 30 min. Samples were then incubated with primary antibody overnight at 4°C, rinsed with PBS, and further incubated in secondary antibodies together with phalloidin for 6 hr. Samples were then mounted with Prolong Gold antifade kit (Invitrogen), cured in the dark at room temperature overnight and imaged with an upright Olympus FluoView FV1000 confocal laser scanning microscope (60X 1.42NA objective).

ABR measurements

The ABR assay was performed using a Tucker Davis Technologies (TDT, Gainsville, FL) workstation (System III). Mice age P28 to P60 were anesthetized by intraperitoneal injection of a ketamine (100 mg/kg)/xylazine (10 mg/kg) cocktail. Anesthetized mice were then placed on a heating pad and electrodes were placed subcutaneously in the vertex, underneath the left ear, and on the back near the tail. Tone stimuli of 4, 5.6, 8, 11.2, 16, 22, 32 and 45.3 kHz were calibrated with a precision microphone system (PS9200Kit, ACO Pacific, USA) using the TDT SigCal software package. The recorded signals were band-pass filtered (300 Hz to 3 kHz) and amplified 100,000 times. The number of acquisition trials was set to 500 averages. Maximum stimulus intensity was set to 95 dB peak SPL with attenuation decreasing from 85 dB to 0 dB SPL at 5 dB SPL intervals. All ABR thresholds were read by second investigator who was blind to the mouse genotype.

Field emission scanning electron microscopy

Cochleas from either P2 or adult (P28-P40) mice were dissected out and immediately immersed in 0.5% glutaraldehyde / 0.1 M sodium cacodylate buffer / 3 mM $CaCl_2$ (pH 7.3) for 2 hr. Adult cochleas were further decalcified in 120 mM EDTA (pH 7.2) for 24 hr. Cochlea coils were dissected out in distilled water. Samples were processed through an OTOTO procedure [112] with modifications. Briefly, samples were washed in the cacodylate dilution buffer three times for 5 min each, fixed in 1% OsO_4 in cacodylate buffer for 1 hr, and washed in H_2O for 5 min three times. The samples then went through 1% freshly prepared tannic acid for 1 hr, then 1% OsO4 for 1 hr, 1% tannic acid for 1 hr, and 1% OsO_4 for 1 hr, with an H_2O wash between steps. Next, samples were washed and processed through the crescent isopropanol series steps (30% isopropanol at room temperature, 50% isopropanol on ice, 70% isopropanol at -20°C, 90% isopropanol slurry on dry ice, 95% isopropanol slurry on dry ice, 100% isopropanol slurry on dry ice), with each step exposition set to 15 min. Sample were then critical point dried, sputter coated with platinum and imaged on a Hitachi S-4800 field emission scanning electron microscope.

Whole-cell patch clamp recording

Organ of Corti epithelia were dissected at P3-P5 in L-15 medium (Life Technologies), placed in glass bottom Petri dishes (WPI Inc.) and cultured for 2–3 days in DMEM/F12 medium (Life Technologies) supplemented with 5% FBS and 10 mg/l ampicillin at 37°C (10% CO_2) as previously described [113]. Experiments were performed at room temperature in L-15 containing the following inorganic salts (in mM): NaCl (137), KCl (5.4), $CaCl_2$ (1.26), $MgCl_2$ (1.0), Na_2HPO_4 (1.0), KH_2PO_4 (0.44), $MgSO_4$ (0.81). Hair cells were observed with an inverted microscope (TE 2000, Nikon) using a 100X 1.3 NA oil-immersion objective lens and DIC optics. Pipettes for whole-cell patch-clamp recordings were filled with intracellular solution containing (in mM): CsCl (140), $MgCl_2$ (2.5), Na_2ATP (2.5), EGTA (1.0), HEPES (5.0). The pipette resistance was typically 4–6 MΩ when measured in the bath. Patch clamp recordings were performed with an AxoPatch 200B amplifier (Molecular Devices) controlled by pClamp 9 software package. Hair cells were held at –60 mV between the short periods of transduction recordings, when the holding potential was temporarily hyperpolarized to –90 mV. All recorded hair cells were located 35–45% away from the apex of the organ of Corti explant.

Hair bundles were deflected using a stiff glass probe, fire-polished to fit the shape of the stereocilia bundle (~5–7 μm). The probe was mounted on a piezo actuator (PA 8/14 SG, Piezosystem Jena), equipped with a strain gauge sensor to provide a direct reading of the probe's axial displacement. The piezo was driven by a custom-made amplifier, providing a rapid step deflection within ~40 μs (10–90% risetime). The angle between the axis of the probe movement and the bottom surface of a dish was kept constant at ~30 degrees.

FM1-43 loading

Organ of Corti epithelia were acutely dissected from P4-P5 mice in L-15 cell culture medium, and either mounted on coverslips using tungsten minutien pins (WPI Inc.) for the experiment, or cultured for an additional 2 days as described above. Following tectorial membrane removal and medium aspiration, FM1-43 solution (2 μM in L-15) was applied to the tissue for 30–60 s, then quickly aspirated; the tissue was rinsed once with L-15 and the excessive dye quenched by a 0.2 mM solution of 4-sulphonato calix[8]arene, sodium salt (SCAS, Biotium) in L-15. The organ of Corti was then observed on an upright Olympus FV1000 confocal microscope, equipped with 60X 1.1 NA water-dipping objective lens.

Supporting Information

S1 Fig. Mouse TRP channel phylogeny. There are 33 genes in six major groups (TRPM, TRPC, TRPV, PKD/TRPP, TRPML and TRPA). Length of line indicates divergence.
(TIF)

S2 Fig. Strategy and validation of *Trpm2* knockout. (a) *Trpm2* conditional knockout strategy. We inserted two LoxP sites to flank a ~1.9 kb region that includes exon 21. A LoxP-FRT-Neo-LoxP-FRT cassette was inserted upstream of exon 21 and the third LoxP site was inserted downstream of exon 21. Exon 21 encodes aa929-985 including the essential fifth transmembrane domain and pore. The deletion also led to a downstream frameshift. Red arrowheads refer to LoxP sites, yellow brackets refer to FRT sites, and green arrows refer to the neomycin resistance gene. Primers used for genotyping and validation are indicated as gray arrows. **(b)** PCR from genomic DNA purified from inner ears of *Trpm2*fl/fl: *Gfi1*-Cre+ mice, *Trpm2*fl/fl: *Gfi1*-Cre- mice, and an age-matched wildtype mouse. *(Left)* PCR results using primer pair TM2cKO15101f and SDL. Lane 1 (*Trpm2*fl/fl:*Gfi1*-Cre+) shows a fused short band (616bp) only from the deleted allele; lane 2 lacking Cre (*Trpm2*fl/fl:*Gfi1*-Cre-) and Lane 3 (wildtype) do not

show it. The fused band was confirmed by Sanger sequencing. (*Middle*) PCR bands at 320 bp (floxed allele) in lane 1 and lane 2, and 259 bp (Wt allele)in lane 3, using primers LOX and SDL, (*Right*) Genotyping for the *Gfi1*-Cre allele. A 1-kb DNA extension ladder was used (5 μl; Invitrogen #10511–012).
(TIF)

S3 Fig. Strategy and validation of *Pkd2* knockout. (a) Exon 9 of the *Pkd2* gene was deleted by flanking the ~2.2 kb targeting region with two LoxP sites. A LoxP-Neo-LoxP cassette was inserted downstream of exon 9 and the third LoxP site was inserted upstream. Exon 9 encodes aa630-671 including the pore domain and most of the sixth transmembrane domain of the Pkd2 channel. Primers used for genotyping and validation are indicated as a gray arrows. **(b)** PCR from genomic DNA purified from inner ears of *Pkd2*$^{fl/fl}$:*Atoh1-Cre*$^{+}$ mice, *Pkd2*$^{fl/fl}$:*Atoh1-Cre*$^{-/-}$ mice, and an age-matched wildtype mouse. *(Left)* PCR results using primer pair PKD2-5940f1 and mPKD2in9R3. Lane 1 (*Pkd2*$^{fl/fl}$:*Atoh1-Cre*$^{+}$) shows a fused short band (344 bp) from the deleted allele and a longer band (>2437 bp) from the genomic DNA cells without Cre activity. The short fused band was confirmed by Sanger sequencing. Lane 2 (*Pkd2*$^{fl/fl}$:*Atoh1-Cre*$^{-}$) shows the same long band as in lane 1 but no short band. Lane 3 shows a band of 2457 bp produced from a wildtype mouse inner ear. (*Middle*) PCR produced bands at 520bp in lane 1 and lane 2, and 468 bp in lane 3 using mPKD2in9F3 and mPKD2inR3. (*Right*) Genotyping of the *Atoh1-Cre* allele. A 1-kb DNA extension ladder was used (5 μl; Invitrogen #10511–012).
(TIF)

S4 Fig. Pkd2 localization and *Pkd2* knockout ABR data, in the second *Pkd2* knockout mouse [83]. (a,a') Antibody labeling (Santa Cruz Biotechnology, #sc-10376) for Pkd2 (red) and phalloidin staining for actin (green) in the heterozygote (*Pkd2*$^{fl/+}$: *Atoh1-Cre*$^{+}$) positive-control cochlea. Pkd2 label is evident in hair-cell kinocilia (arrowheads) and some supporting cell primary cilia (arrows). **(b,b')** *Pkd2*$^{fl/fl}$: *Atoh1-Cre*$^{+}$ knockout cochlea. Pkd2 label is absent from hair cell kinocilia but not from supporting cell cilia. **(c-c')** In vestibular hair cells of heterozygote mice, Pkd2 label is also in kinocilia. **(d)** ABR thresholds in response to pure tone stimuli. *Pkd2*$^{fl/fl}$: *Atoh1-Cre*$^{+}$ knockout mice show normal hearing. Data are mean ± SEM.
(TIF)

S5 Fig. *Pkd2l2* knockout. The generation of the *Pkd2l2* knockout mouse, based on information from The Jackson Laboratory (*Pkd2l2*^{tm1Dgen}/J; stock #005829; https://www.jax.org/strain/005829). A bacterial lacZ gene fused with a neomycin resistance gene replaced ~ 1.8 kb genomic sequence extending from the 3' part of exon 3 to the 5' part of exon 4. Thus the endogenous promoter drove the expression of beta-galactosidase.
(TIF)

Acknowledgments

Author Contributions

Conceived and designed the experiments: XW AAI PDN RMW MAV DPC. Performed the experiments: XW AAI PDN RMW. Analyzed the data: XW AAI PDN RMW DPC. Contributed reagents/materials/analysis tools: MG-G TW JZ. Wrote the paper: XW AAI DPC.

References

1. Hudspeth AJ, Corey DP (1977) Sensitivity, polarity, and conductance change in the response of vertebrate hair cells to controlled mechanical stimuli. Proc Natl Acad Sci U S A 74: 2407–2411. PMID: 329282

2. Corey DP, Hudspeth AJ (1979) Response latency of vertebrate hair cells. Biophys J 26: 499–506. PMID: 318064

3. Corey DP, Hudspeth AJ (1979) Ionic basis of the receptor potential in a vertebrate hair cell. Nature 281: 675–677. PMID: 45121

4. Ohmori H (1985) Mechano-electrical transduction currents in isolated vestibular hair cells of the chick. J Physiol 359: 189–217. PMID: 2582113

5. Lumpkin EA, Marquis RE, Hudspeth AJ (1997) The selectivity of the hair cell's mechanoelectrical-transduction channel promotes Ca2+ flux at low Ca2+ concentrations. Proc Natl Acad Sci U S A 94: 10997–11002. PMID: 9380748

6. Crawford AC, Evans MG, Fettiplace R (1991) The actions of calcium on the mechano-electrical transducer current of turtle hair cells. J Physiol 434: 369–398. PMID: 1708822

7. Kimitsuki T, Nakagawa T, Hisashi K, Komune S, Komiyama S (1996) Gadolinium blocks mechano-electric transducer current in chick cochlear hair cells. Hear Res 101: 75–80. PMID: 8951434

8. Farris HE, LeBlanc CL, Goswami J, Ricci AJ (2004) Probing the pore of the auditory hair cell mechanotransducer channel in turtle. J Physiol 558: 769–792. PMID: 15181168

9. Geleoc GS, Lennan GW, Richardson GP, Kros CJ (1997) A quantitative comparison of mechanoelectrical transduction in vestibular and auditory hair cells of neonatal mice. Proc Biol Sci 264: 611–621. PMID: 9149428

10. Ricci AJ, Crawford AC, Fettiplace R (2003) Tonotopic variation in the conductance of the hair cell mechanotransducer channel. Neuron 40: 983–990. PMID: 14659096

11. Beurg M, Evans MG, Hackney CM, Fettiplace R (2006) A large-conductance calcium-selective mechanotransducer channel in mammalian cochlear hair cells. J Neurosci 26: 10992–11000. PMID: 17065441

12. Pan B, Geleoc GS, Asai Y, Horwitz GC, Kurima K, Ishikawa K, et al. (2013) TMC1 and TMC2 are components of the mechanotransduction channel in hair cells of the mammalian inner ear. Neuron 79: 504–515. doi: 10.1016/j.neuron.2013.06.019 PMID: 23871232

13. Rusch A, Kros CJ, Richardson GP (1994) Block by amiloride and its derivatives of mechano-electrical transduction in outer hair cells of mouse cochlear cultures. J Physiol 474: 75–86. PMID: 7516972

14. Gale JE, Marcotti W, Kennedy HJ, Kros CJ, Richardson GP (2001) FM1-43 dye behaves as a permeant blocker of the hair-cell mechanotransducer channel. J Neurosci 21: 7013–7025. PMID: 11549711

15. Kroese AB, Das A, Hudspeth AJ (1989) Blockage of the transduction channels of hair cells in the bullfrog's sacculus by aminoglycoside antibiotics. Hear Res 37: 203–217. PMID: 2468634

16. Ricci A (2002) Differences in mechano-transducer channel kinetics underlie tonotopic distribution of fast adaptation in auditory hair cells. J Neurophysiol 87: 1738–1748. PMID: 11929895

17. Marcotti W, van Netten SM, Kros CJ (2005) The aminoglycoside antibiotic dihydrostreptomycin rapidly enters mouse outer hair cells through the mechano-electrical transducer channels. J Physiol 567: 505–521. PMID: 15994187

18. Pan B, Waguespack J, Schnee ME, LeBlanc C, Ricci AJ (2012) Permeation properties of the hair cell mechanotransducer channel provide insight into its molecular structure. J Neurophysiol 107: 2408–2420. doi: 10.1152/jn.01178.2011 PMID: 22323630

19. Vollrath MA, Kwan KY, Corey DP (2007) The micromachinery of mechanotransduction in hair cells. Annu Rev Neurosci 30: 339–365. PMID: 17428178

20. Cuajungco MP, Grimm C, Heller S (2007) TRP channels as candidates for hearing and balance abnormalities in vertebrates. Biochim Biophys Acta 1772: 1022–1027. PMID: 17300924

21. Fettiplace R (2009) Defining features of the hair cell mechanoelectrical transducer channel. Pflugers Arch 458: 1115–1123. doi: 10.1007/s00424-009-0683-x PMID: 19475417

22. Geleoc GS, Holt JR (2003) Developmental acquisition of sensory transduction in hair cells of the mouse inner ear. Nat Neurosci 6: 1019–1020. PMID: 12973354

23. Lelli A, Asai Y, Forge A, Holt JR, Geleoc GS (2009) Tonotopic gradient in the developmental acquisition of sensory transduction in outer hair cells of the mouse cochlea. J Neurophysiol 101: 2961–2973. doi: 10.1152/jn.00136.2009 PMID: 19339464

24. Asai Y, Holt JR, Geleoc GS (2010) A quantitative analysis of the spatiotemporal pattern of transient receptor potential gene expression in the developing mouse cochlea. J Assoc Res Otolaryngol 11: 27–37. doi: 10.1007/s10162-009-0193-8 PMID: 19834762

25. Scheffer DI, Shen J, Corey DP, Chen ZY (2015) Gene Expression by Mouse Inner Ear Hair Cells during Development. J Neurosci 35: 6366–6380. doi: 10.1523/JNEUROSCI.5126-14.2015 PMID: 25904789

26. Caterina MJ, Schumacher MA, Tominaga M, Rosen TA, Levine JD, Julius D (1997) The capsaicin receptor: a heat-activated ion channel in the pain pathway. Nature 389: 816–824. PMID: 9349813

27. Zitt C, Obukhov AG, Strubing C, Zobel A, Kalkbrenner F, Luckhoff A, et al. (1997) Expression of TRPC3 in Chinese hamster ovary cells results in calcium-activated cation currents not related to store depletion. J Cell Biol 138: 1333–1341. PMID: 9298988

28. Chen XZ, Vassilev PM, Basora N, Peng JB, Nomura H, Segal Y, et al. (1999) Polycystin-L is a calcium-regulated cation channel permeable to calcium ions. Nature 401: 383–386. PMID: 10517637

29. Hofmann T, Obukhov AG, Schaefer M, Harteneck C, Gudermann T, Schultz G (1999) Direct activation of human TRPC6 and TRPC3 channels by diacylglycerol. Nature 397: 259–263. PMID: 9930701

30. Nilius B, Vennekens R, Prenen J, Hoenderop JG, Bindels RJ, Droogmans G (2000) Whole-cell and single channel monovalent cation currents through the novel rabbit epithelial Ca2+ channel ECaC. J Physiol 527 Pt 2: 239–248. PMID: 10970426

31. Strotmann R, Harteneck C, Nunnenmacher K, Schultz G, Plant TD (2000) OTRPC4, a nonselective cation channel that confers sensitivity to extracellular osmolarity. Nat Cell Biol 2: 695–702. PMID: 11025659

32. Vennekens R, Hoenderop JG, Prenen J, Stuiver M, Willems PH, Droogmans G, et al. (2000) Permeation and gating properties of the novel epithelial Ca(2+) channel. J Biol Chem 275: 3963–3969. PMID: 10660551

33. Nadler MJ, Hermosura MC, Inabe K, Perraud AL, Zhu Q, Stokes AJ, et al. (2001) LTRPC7 is a Mg. ATP-regulated divalent cation channel required for cell viability. Nature 411: 590–595. PMID: 11385574

34. Perraud AL, Fleig A, Dunn CA, Bagley LA, Launay P, Schmitz C, et al. (2001) ADP-ribose gating of the calcium-permeable LTRPC2 channel revealed by Nudix motif homology. Nature 411: 595–599. PMID: 11385575

35. Runnels LW, Yue L, Clapham DE (2001) TRP-PLIK, a bifunctional protein with kinase and ion channel activities. Science 291: 1043–1047. PMID: 11161216

36. Sano Y, Inamura K, Miyake A, Mochizuki S, Yokoi H, Matsushime H, et al. (2001) Immunocyte Ca2+ influx system mediated by LTRPC2. Science 293: 1327–1330. PMID: 11509734

37. Strubing C, Krapivinsky G, Krapivinsky L, Clapham DE (2001) TRPC1 and TRPC5 form a novel cation channel in mammalian brain. Neuron 29: 645–655. PMID: 11301024

38. Voets T, Prenen J, Fleig A, Vennekens R, Watanabe H, Hoenderop JG, et al. (2001) CaT1 and the calcium release-activated calcium channel manifest distinct pore properties. J Biol Chem 276: 47767–47770. PMID: 11687570

39. Yue L, Peng JB, Hediger MA, Clapham DE (2001) CaT1 manifests the pore properties of the calcium-release-activated calcium channel. Nature 410: 705–709. PMID: 11287959

40. Gonzalez-Perrett S, Batelli M, Kim K, Essafi M, Timpanaro G, Moltabetti N, et al. (2002) Voltage dependence and pH regulation of human polycystin-2-mediated cation channel activity. J Biol Chem 277: 24959–24966. PMID: 11991947

41. LaPlante JM, Falardeau J, Sun M, Kanazirska M, Brown EM, Slaugenhaupt SA, et al. (2002) Identification and characterization of the single channel function of human mucolipin-1 implicated in mucolipidosis type IV, a disorder affecting the lysosomal pathway. FEBS Lett 532: 183–187. PMID: 12459486

42. Voets T, Prenen J, Vriens J, Watanabe H, Janssens A, Wissenbach U, et al. (2002) Molecular determinants of permeation through the cation channel TRPV4. J Biol Chem 277: 33704–33710. PMID: 12093812

43. Watanabe H, Vriens J, Suh SH, Benham CD, Droogmans G, Nilius B (2002) Heat-evoked activation of TRPV4 channels in a HEK293 cell expression system and in native mouse aorta endothelial cells. J Biol Chem 277: 47044–47051. PMID: 12354759

44. Xu H, Ramsey IS, Kotecha SA, Moran MM, Chong JA, Lawson D, et al. (2002) TRPV3 is a calcium-permeable temperature-sensitive cation channel. Nature 418: 181–186. PMID: 12077604

45. Grimm C, Kraft R, Sauerbruch S, Schultz G, Harteneck C (2003) Molecular and functional characterization of the melastatin-related cation channel TRPM3. J Biol Chem 278: 21493–21501. PMID: 12672799

46. Heiner I, Eisfeld J, Halaszovich CR, Wehage E, Jungling E, Zitt C, et al. (2003) Expression profile of the transient receptor potential (TRP) family in neutrophil granulocytes: evidence for currents through long TRP channel 2 induced by ADP-ribose and NAD. Biochem J 371: 1045–1053. PMID: 12564954

47. Hofmann T, Chubanov V, Gudermann T, Montell C (2003) TRPM5 is a voltage-modulated and Ca(2 +)-activated monovalent selective cation channel. Curr Biol 13: 1153–1158. PMID: 12842017

48. Luo Y, Vassilev PM, Li X, Kawanabe Y, Zhou J (2003) Native polycystin 2 functions as a plasma membrane Ca2+-permeable cation channel in renal epithelia. Mol Cell Biol 23: 2600–2607. PMID: 12640140

49. Nilius B, Prenen J, Droogmans G, Voets T, Vennekens R, Freichel M, et al. (2003) Voltage dependence of the Ca2+-activated cation channel TRPM4. J Biol Chem 278: 30813–30820. PMID: 12799367

50. Prawitt D, Monteilh-Zoller MK, Brixel L, Spangenberg C, Zabel B, Fleig A, et al. (2003) TRPM5 is a transient Ca2+-activated cation channel responding to rapid changes in [Ca2+]i. Proc Natl Acad Sci U S A 100: 15166–15171. PMID: 14634208

51. Chung MK, Lee H, Mizuno A, Suzuki M, Caterina MJ (2004) 2-aminoethoxydiphenyl borate activates and sensitizes the heat-gated ion channel TRPV3. J Neurosci 24: 5177–5182. PMID: 15175387

52. LaPlante JM, Ye CP, Quinn SJ, Goldin E, Brown EM, Slaugenhaupt SA, et al. (2004) Functional links between mucolipin-1 and Ca2+-dependent membrane trafficking in mucolipidosis IV. Biochem Biophys Res Commun 322: 1384–1391. PMID: 15336987

53. Launay P, Cheng H, Srivatsan S, Penner R, Fleig A, Kinet JP (2004) TRPM4 regulates calcium oscillations after T cell activation. Science 306: 1374–1377. PMID: 15550671

54. Shi J, Mori E, Mori Y, Mori M, Li J, Ito Y, et al. (2004) Multiple regulation by calcium of murine homologues of transient receptor potential proteins TRPC6 and TRPC7 expressed in HEK293 cells. J Physiol 561: 415–432. PMID: 15579537

55. Grimm C, Kraft R, Schultz G, Harteneck C (2005) Activation of the melastatin-related cation channel TRPM3 by D-erythro-sphingosine [corrected]. Mol Pharmacol 67: 798–805. PMID: 15550678

56. Nagata K, Duggan A, Kumar G, Garcia-Anoveros J (2005) Nociceptor and hair cell transducer properties of TRPA1, a channel for pain and hearing. J Neurosci 25: 4052–4061. PMID: 15843607

57. Nilius B, Prenen J, Janssens A, Owsianik G, Wang C, Zhu MX, et al. (2005) The selectivity filter of the cation channel TRPM4. J Biol Chem 280: 22899–22906. PMID: 15845551

58. Oberwinkler J, Lis A, Giehl KM, Flockerzi V, Philipp SE (2005) Alternative splicing switches the divalent cation selectivity of TRPM3 channels. J Biol Chem 280: 22540–22548. PMID: 15824111

59. Li M, Jiang J, Yue L (2006) Functional characterization of homo- and heteromeric channel kinases TRPM6 and TRPM7. J Gen Physiol 127: 525–537. PMID: 16636202

60. Togashi K, Hara Y, Tominaga T, Higashi T, Konishi Y, Mori Y, et al. (2006) TRPM2 activation by cyclic ADP-ribose at body temperature is involved in insulin secretion. Embo J 25: 1804–1815. PMID: 16601673

61. Grimm C, Cuajungco MP, van Aken AF, Schnee M, Jors S, Kros CJ, et al. (2007) A helix-breaking mutation in TRPML3 leads to constitutive activity underlying deafness in the varitint-waddler mouse. Proc Natl Acad Sci U S A 104: 19583–19588. PMID: 18048323

62. Xu H, Delling M, Li L, Dong X, Clapham DE (2007) Activating mutation in a mucolipin transient receptor potential channel leads to melanocyte loss in varitint-waddler mice. Proc Natl Acad Sci U S A 104: 18321–18326. PMID: 17989217

63. Kim HJ, Li Q, Tjon-Kon-Sang S, So I, Kiselyov K, Soyombo AA, et al. (2008) A novel mode of TRPML3 regulation by extracytosolic pH absent in the varitint-waddler phenotype. Embo J 27: 1197–1205. doi: 10.1038/emboj.2008.56 PMID: 18369318

64. Nagata K, Zheng L, Madathany T, Castiglioni AJ, Bartles JR, Garcia-Anoveros J (2008) The varitint-waddler (Va) deafness mutation in TRPML3 generates constitutive, inward rectifying currents and causes cell degeneration. Proc Natl Acad Sci U S A 105: 353–358. PMID: 18162548

65. Bobkov YV, Corey EA, Ache BW (2011) The pore properties of human nociceptor channel TRPA1 evaluated in single channel recordings. Biochim Biophys Acta 1808: 1120–1128. doi: 10.1016/j.bbamem.2010.12.024 PMID: 21195050

66. Zhang X, Li X, Xu H (2012) Phosphoinositide isoforms determine compartment-specific ion channel activity. Proc Natl Acad Sci U S A 109: 11384–11389. doi: 10.1073/pnas.1202194109 PMID: 22733759

67. DeCaen PG, Delling M, Vien TN, Clapham DE (2013) Direct recording and molecular identification of the calcium channel of primary cilia. Nature 504: 315–318. doi: 10.1038/nature12832 PMID: 24336289

68. Clapham DE, DeCaen P, Carvacho I, Chaudhuri D, Doerner JF, Julius D, et al. (2016) IUPHAR/BPS Guide to PHARMACOLOGY. http://wwwguidetopharmacologyorg/GRAC/FamilyDisplayForward? familyId=78.

69. Liu H, Pecka JL, Zhang Q, Soukup GA, Beisel KW, He DZ (2014) Characterization of transcriptomes of cochlear inner and outer hair cells. J Neurosci 34: 11085–11095. doi: 10.1523/JNEUROSCI.1690-14.2014 PMID: 25122905

70. Kwan KY, Allchorne AJ, Vollrath MA, Christensen AP, Zhang DS, Woolf CJ, et al. (2006) TRPA1 contributes to cold, mechanical, and chemical nociception but is not essential for hair-cell transduction. Neuron 50: 277–289. PMID: 16630838

71. Sexton JE, Desmonds T, Quick K, Taylor R, Abramowitz J, Forge A, et al. (2016) The contribution of TRPC1, TRPC3, TRPC5 and TRPC6 to touch and hearing. Neurosci Lett 610: 36–42. doi: 10.1016/j. neulet.2015.10.052 PMID: 26520460

72. Tabuchi K, Suzuki M, Mizuno A, Hara A (2005) Hearing impairment in TRPV4 knockout mice. Neurosci Lett 382: 304–308. PMID: 15925108

73. Gerka-Stuyt J, Au A, Peachey NS, Alagramam KN (2013) Transient receptor potential melastatin 1: a hair cell transduction channel candidate. PLoS One 8: e77213. doi: 10.1371/journal.pone.0077213 PMID: 24146970

74. Alagramam KN, Goodyear RJ, Geng R, Furness DN, van Aken AF, Marcotti W, et al. (2011) Mutations in protocadherin 15 and cadherin 23 affect tip links and mechanotransduction in mammalian sensory hair cells. PLoS One 6: e19183. doi: 10.1371/journal.pone.0019183 PMID: 21532990

75. Yang H, Gan J, Xie X, Deng M, Feng L, Chen X, et al. (2010) Gfi1-Cre knock-in mouse line: A tool for inner ear hair cell-specific gene deletion. Genesis 48: 400–406. doi: 10.1002/dvg.20632 PMID: 20533399

76. Meyers JR, MacDonald RB, Duggan A, Lenzi D, Standaert DG, Corwin JT, et al. (2003) Lighting up the senses: FM1-43 loading of sensory cells through nonselective ion channels. J Neurosci 23: 4054–4065. PMID: 12764092

77. Yao G, Luo C, Harvey M, Wu M, Schreiber TH, Du Y, et al. (2015) Disruption of Polycystin-L causes Hippocampal Hyperexcitability. Hum Mol Genet.

78. Tsiokas L, Kim E, Arnould T, Sukhatme VP, Walz G (1997) Homo- and heterodimeric interactions between the gene products of PKD1 and PKD2. Proc Natl Acad Sci U S A 94: 6965–6970. PMID: 9192675

79. Newby LJ, Streets AJ, Zhao Y, Harris PC, Ward CJ, Ong AC (2002) Identification, characterization, and localization of a novel kidney polycystin-1-polycystin-2 complex. J Biol Chem 277: 20763–20773. PMID: 11901144

80. Murakami M, Ohba T, Xu F, Shida S, Satoh E, Ono K, et al. (2005) Genomic organization and functional analysis of murine PKD2L1. J Biol Chem 280: 5626–5635. PMID: 15548533

81. Ishimaru Y, Katano Y, Yamamoto K, Akiba M, Misaka T, Roberts RW, et al. (2010) Interaction between PKD1L3 and PKD2L1 through their transmembrane domains is required for localization of PKD2L1 at taste pores in taste cells of circumvallate and foliate papillae. Faseb J 24: 4058–4067. doi: 10.1096/fj.10-162925 PMID: 20538909

82. Matei V, Pauley S, Kaing S, Rowitch D, Beisel KW, Morris K, et al. (2005) Smaller inner ear sensory epithelia in Neurog 1 null mice are related to earlier hair cell cycle exit. Dev Dyn 234: 633–650. PMID: 16145671

83. Garcia-Gonzalez MA, Outeda P, Zhou Q, Zhou F, Menezes LF, Qian F, et al. (2010) Pkd1 and Pkd2 are required for normal placental development. PLoS One 5.

84. Huang AL, Chen X, Hoon MA, Chandrashekar J, Guo W, Trankner D, et al. (2006) The cells and logic for mammalian sour taste detection. Nature 442: 934–938. PMID: 16929298

85. Ishimaru Y, Inada H, Kubota M, Zhuang H, Tominaga M, Matsunami H (2006) Transient receptor potential family members PKD1L3 and PKD2L1 form a candidate sour taste receptor. Proc Natl Acad Sci U S A 103: 12569–12574. PMID: 16891422

86. Ye W, Chang RB, Bushman JD, Tu YH, Mulhall EM, Wilson CE, et al. (2016) The K+ channel KIR2.1 functions in tandem with proton influx to mediate sour taste transduction. Proc Natl Acad Sci U S A 113: E229–238. doi: 10.1073/pnas.1514282112 PMID: 26627720

87. Nelson TM, Lopezjimenez ND, Tessarollo L, Inoue M, Bachmanov AA, Sullivan SL (2010) Taste function in mice with a targeted mutation of the pkd1l3 gene. Chem Senses 35: 565–577. doi: 10.1093/chemse/bjq070 PMID: 20605874

88. Eijkelkamp N, Quick K, Wood JN (2013) Transient receptor potential channels and mechanosensation. Annu Rev Neurosci 36: 519–546. doi: 10.1146/annurev-neuro-062012-170412 PMID: 23750514

89. Lin SY, Corey DP (2005) TRP channels in mechanosensation. Curr Opin Neurobiol 15: 350–357. PMID: 15922584

90. Christensen AP, Corey DP (2007) TRP channels in mechanosensation: direct or indirect activation? Nat Rev Neurosci 8: 510–521. PMID: 17585304

91. Di Palma F, Belyantseva IA, Kim HJ, Vogt TF, Kachar B, Noben-Trauth K (2002) Mutations in Mcoln3 associated with deafness and pigmentation defects in varitint-waddler (Va) mice. Proc Natl Acad Sci U S A 99: 14994–14999. PMID: 12403827

92. van Aken AF, Atiba-Davies M, Marcotti W, Goodyear RJ, Bryant JE, Richardson GP, et al. (2008) TRPML3 mutations cause impaired mechano-electrical transduction and depolarization by an inward-rectifier cation current in auditory hair cells of varitint-waddler mice. J Physiol 586: 5403–5418. doi: 10.1113/jphysiol.2008.156992 PMID: 18801844

93. Jors S, Grimm C, Becker L, Heller S (2010) Genetic inactivation of Trpml3 does not lead to hearing and vestibular impairment in mice. PLoS One 5: e14317. doi: 10.1371/journal.pone.0014317 PMID: 21179200

94. Wang W, Zhang X, Gao Q, Xu H (2014) TRPML1: an ion channel in the lysosome. Handb Exp Pharmacol 222: 631–645. doi: 10.1007/978-3-642-54215-2_24 PMID: 24756723

95. Hoenderop JG, van Leeuwen JP, van der Eerden BC, Kersten FF, van der Kemp AW, Merillat AM, et al. (2003) Renal Ca2+ wasting, hyperabsorption, and reduced bone thickness in mice lacking TRPV5. J Clin Invest 112: 1906–1914. PMID: 14679186

96. Delling M, DeCaen PG, Doerner JF, Febvay S, Clapham DE (2013) Primary cilia are specialized calcium signalling organelles. Nature 504: 311–314. doi: 10.1038/nature12833 PMID: 24336288

97. Nauli SM, Alenghat FJ, Luo Y, Williams E, Vassilev P, Li X, et al. (2003) Polycystins 1 and 2 mediate mechanosensation in the primary cilium of kidney cells. Nat Genet 33: 129–137. PMID: 12514735

98. Kottgen M, Buchholz B, Garcia-Gonzalez MA, Kotsis F, Fu X, Doerken M, et al. (2008) TRPP2 and TRPV4 form a polymodal sensory channel complex. J Cell Biol 182: 437–447. doi: 10.1083/jcb.200805124 PMID: 18695040

99. Du J, Ma X, Shen B, Huang Y, Birnbaumer L, Yao X (2014) TRPV4, TRPC1, and TRPP2 assemble to form a flow-sensitive heteromeric channel. Faseb J 28: 4677–4685. doi: 10.1096/fj.14-251652 PMID: 25114176

100. Delling M, Indzhykulian AA, Liu X, Li Y, Xie T, Corey DP, et al. (2016) Primary cilia are not calcium-responsive mechanosensors. Nature 531: 656–660. doi: 10.1038/nature17426 PMID: 27007841

101. Shin JB, Krey JF, Hassan A, Metlagel Z, Tauscher AN, Pagana JM, et al. (2013) Molecular architecture of the chick vestibular hair bundle. Nat Neurosci 16: 365–374. doi: 10.1038/nn.3312 PMID: 23334578

102. LopezJimenez ND, Cavenagh MM, Sainz E, Cruz-Ithier MA, Battey JF, Sullivan SL (2006) Two members of the TRPP family of ion channels, Pkd1l3 and Pkd2l1, are co-expressed in a subset of taste receptor cells. J Neurochem 98: 68–77. PMID: 16805797

103. Ishii S, Misaka T, Kishi M, Kaga T, Ishimaru Y, Abe K (2009) Acetic acid activates PKD1L3-PKD2L1 channel—a candidate sour taste receptor. Biochem Biophys Res Commun 385: 346–350. doi: 10.1016/j.bbrc.2009.05.069 PMID: 19464260

104. Steigelman KA, Lelli A, Wu X, Gao J, Lin S, Piontek K, et al. (2011) Polycystin-1 is required for stereocilia structure but not for mechanotransduction in inner ear hair cells. J Neurosci 31: 12241–12250. doi: 10.1523/JNEUROSCI.6531-10.2011 PMID: 21865467

105. Yu Y, Ulbrich MH, Li MH, Buraei Z, Chen XZ, Ong AC, et al. (2009) Structural and molecular basis of the assembly of the TRPP2/PKD1 complex. Proc Natl Acad Sci U S A 106: 11558–11563. doi: 10.1073/pnas.0903684106 PMID: 19556541

106. Corey DP, Garcia-Anoveros J, Holt JR, Kwan KY, Lin SY, Vollrath MA, et al. (2004) TRPA1 is a candidate for the mechanosensitive transduction channel of vertebrate hair cells. Nature 432: 723–730. PMID: 15483558

107. Liman ER, Corey DP, Dulac C (1999) TRP2: a candidate transduction channel for mammalian pheromone sensory signaling. Proc Natl Acad Sci U S A 96: 5791–5796. PMID: 10318963

108. Stowers L, Holy TE, Meister M, Dulac C, Koentges G (2002) Loss of sex discrimination and male-male aggression in mice deficient for TRP2. Science 295: 1493–1500. PMID: 11823606

109. Liman ER, Innan H (2003) Relaxed selective pressure on an essential component of pheromone transduction in primate evolution. Proc Natl Acad Sci U S A 100: 3328–3332. PMID: 12631698

110. Low SE, Amburgey K, Horstick E, Linsley J, Sprague SM, Cui WW, et al. (2011) TRPM7 is required within zebrafish sensory neurons for the activation of touch-evoked escape behaviors. J Neurosci 31: 11633–11644. doi: 10.1523/JNEUROSCI.4950-10.2011 PMID: 21832193

111. Liedtke W, Tobin DM, Bargmann CI, Friedman JM (2003) Mammalian TRPV4 (VR-OAC) directs behavioral responses to osmotic and mechanical stimuli in Caenorhabditis elegans. Proc Natl Acad Sci U S A 100 Suppl 2: 14531–14536. PMID: 14581619

112. Forge A, Nevill G, Zajic G, Wright A (1992) Scanning electron microscopy of the mammalian organ of Corti: assessment of preparative procedures. Scanning Microsc 6: 521–534; discussion 534–525. PMID: 1462137

113. Indzhykulian AA, Stepanyan R, Nelina A, Spinelli KJ, Ahmed ZM, Belyantseva IA, et al. (2013) Molecular remodeling of tip links underlies mechanosensory regeneration in auditory hair cells. PLoS Biol 11: e1001583. doi: 10.1371/journal.pbio.1001583 PMID: 23776407